AIAA JOURNAL
Vol. 44, No. 5, May 2006

Rotor-Stator Interaction Noise in Swirling Flow: Stator Sweep and Lean Effects

A. J. Cooper*
University of Warwick, Coventry, England CV4 7AL, United Kingdom
and
N. Peake†
University of Cambridge, Cambridge, England CB3 0WA, United Kingdom

An asymptotic technique in the limit of large blade and vane number is employed to study the interaction in mean swirling flow of an unsteady rotor wake with a stator row downstream. The effect of various stator characteristics, including stator sweep, lean and number of vanes, on the tone noise radiated upstream is investigated. The important effects of mean swirl are included in both the rotor wake evolution and the construction of the upstream-radiated sound field. Specifically, we construct the first term in the series expansion of the upstream unsteady pressure in inverse powers of the blade count. We show that sweep and lean in suitable combination (positive sweep and positive lean) can lead to this first term becoming zero, so that the upstream radiation is then approximated by the next (smaller) term in the series, and is therefore necessarily reduced. A simple criterion, based on the form of the incident wake at the stator leading edge, which leads to this first term becoming zero, is identified. This provides a very efficient method for assessing the impact of sweep and lean over a wide range of operating conditions. The analytical nature of the model allows the physical mechanism behind the effectiveness of sweep and lean to be identified.

Nomenclature

A	=	component of local cascade gust amplitude
$\boldsymbol{A}$	=	vector of vortical velocity amplitudes
$\mathcal{A}$	=	component of total velocity amplitude
a	=	sound speed
B	=	number of rotor blades
b	=	stator blade semichord length
$\hat{c}$	=	pressure coefficient for duct acoustic field
d, s	=	leading-edge separation along X and Y axes
$\boldsymbol{e}$	=	unit vector
F	=	complex disturbance potential for cascade
h	=	unsteady velocity potential ahead of cascade
j, n	=	indices
$K, \tilde{K}$	=	aerodynamic reduced frequency in stationary and moving frames
k	=	wave number
M	=	Mach number
$\boldsymbol{M}$	=	wake evolution matrix
$m, \hat{m}$	=	azimuthal mode number of incoming gust and acoustic field
N	=	integer
P	=	total cross-sectionally averaged pressure field
$\mathcal{P}$	=	pressure eigenfunctions for duct acoustic field
p	=	unsteady pressure
R	=	modal coefficients of cascade unsteady velocity potential
r	=	duct radius
$\boldsymbol{S}, \boldsymbol{T}$	=	transformation matrices for sweep and lean
t	=	time
U	=	component of mean velocity field
$\boldsymbol{U}$	=	mean velocity field
$\boldsymbol{u}$	=	vortical part of unsteady velocity perturbation
$\boldsymbol{u}'$	=	unsteady velocity perturbation
V	=	number of stator blades
$\boldsymbol{V}$	=	total velocity field
X, Y, Z	=	local cascade Cartesian coordinates
x, r, θ	=	cylindrical coordinates
β	=	$\sqrt{(1-M^2)}$
γ	=	flow angle in duct
Δ	=	stator blade leading-edge separation
δ	=	mean loading parameter
ζ	=	sweep or lean angle in duct
κ	=	effective sweep or lean angle in cascade system
$\boldsymbol{\xi}$	=	mean vorticity in duct
ρ	=	mean density
Φ	=	unsteady velocity potential
ϕ, ψ	=	Prandtl–Glauert potential, stream-function coordinates
φ	=	potential velocity amplitude
χ	=	stagger angle
Ω	=	angular velocity of fan
ω	=	frequency

Subscripts

c, d	=	cascade and duct systems
h, t	=	hub and tip locations
i	=	incompressible
m	=	evaluated at $\omega = m\Omega$
S	=	stator location
s, l	=	sweep and lean
X, Y, Z	=	components in local cascade system
x, r, θ	=	components in duct
0	=	local quantity
∞	=	reference value

Superscripts

T	=	vector transpose
$*$	=	dimensional quantity

Received 16 October 2003; revision received 30 June 2005; accepted for publication 23 August 2005.

*Royal Society University Research Fellow, School of Engineering.
†Professor, Department of Applied Mathematics and Theoretical Physics. Member AIAA.

Introduction

NOISE reduction is now one of the major issues in aeroengine design. In modern high-bypass-ratio turbofan systems much of the noise is generated by the fan, particularly by the interaction of rotor-wake disturbances with downstream vanes. A significant component of this rotor-stator interaction noise is tone noise, which appears at multiples of the blade passing frequency (BPF) and is caused by the impingement of the periodic fan wakes with the stator vanes. There is also an important broadband component produced by, among other things, the interaction of rotor-wake turbulence with the stator. Stator design characteristics, such as the number of stator vanes, vane stagger angle, geometry, and position, can have a significant effect on the noise generated. It is not generally practical to perform a comprehensive experimental investigation into the effects of stator design because each configuration requires a purpose-built stator. Numerical schemes also involve significant changes to the computation for each stator configuration. With this in mind an analytically based noise prediction scheme, developed in Ref. 1, is used to assess the effects of a wide variety of stator designs with the aim of providing design criteria. The value of this type of model lies in the efficiency with which a range of configurations can be investigated and the ability to extract underlying physical mechanisms.

Rotor-stator interaction tone noise is strongly dependent on the orientation of the wakes to the stator leading edge. In particular, tone noise can be reduced by increasing the rotor-stator spacing to enhance the wake skewing brought about by propagation of the wakes through mean swirling flow.[1,2] However, to avoid weight penalties and possible degradation in performance brought about by increasing the length of the duct, the effects of wake skewing can be maximized by applying sweep and lean to the stator. Sweep describes the axial displacement of the stator with radius, such that for positive sweep the stator at the tip lies farther downstream than at the hub. Lean is the circumferential displacement of the stator vane from its radial position, with positive lean taken to be in the direction of fan rotation. Stator sweep and lean are defined by the angles ζ_s and ζ_l, respectively, and the orientation of the stator in each case is shown in Fig. 1. A number of previous investigations into sweep[3–8] and lean[9–11] have suggested the possibility of tone noise reduction, and more recently an experimental study[12] carried out a series of experimental tests on an advanced high-bypass fan stage. Budget considerations restricted that investigation to four stator designs: a radial stator in forward and aft locations as well as a swept stator and a swept-and-leaned stator. Their results indicated that significant reductions in noise levels could be achieved over a wide range of operating conditions, and in certain cases sweep and lean could bring about complete elimination of some BPF tones. These experimental results prompted an analytical investigation into design selection criteria[2] aimed at identifying sweep and lean configurations that maximize tone noise reduction. This study demonstrated general trends that were in agreement with experimental observations and identified an optimal design combination of positive sweep and positive lean for maximum noise reduction.

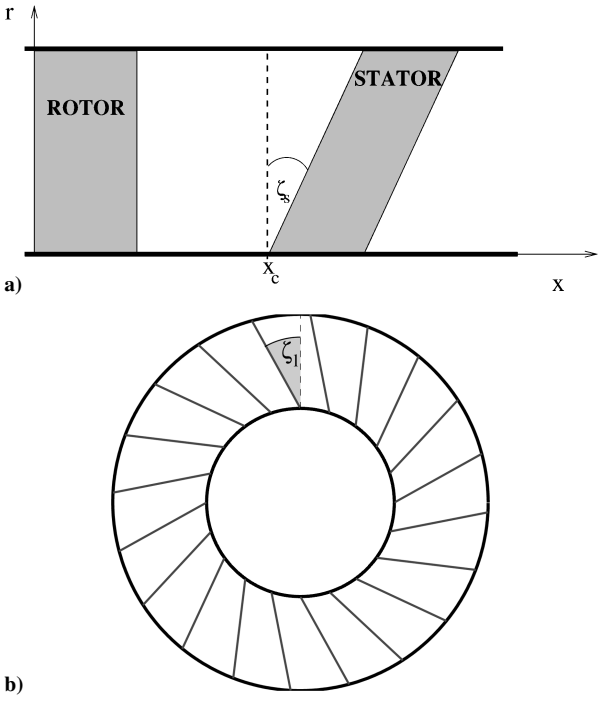

Fig. 1 Stator configurations: a) side view showing sweep angle ζ_s and b) front view showing lean angle ζ_l (positive in direction of fan rotation).

Previous analytically based models have not included the important effects of mean swirling flow between the rotor and the stator. Swirl affects both the rotor-wake evolution and the upstream-radiated sound field and is required for accurate representation of the upstream-radiated noise. Recently[1] an asymptotic model based on a large fan-blade number (equivalently a high-frequency analysis) that systematically includes the effects of swirl on the complete rotor-stator interaction process was developed. The form of the wake profile at the stator blade leading edges has been identified as a critical factor in the noise-generation process,[1,2] and the ability to account accurately for the wake profile when sweep and lean are applied is crucial to any noise prediction scheme. Swirl is also an important factor for the prediction of the upstream noise field because it affects the number of cut-on, or propagating, acoustic modes in the duct. Computational interaction noise models that include the effects of swirl in an annular duct have also been developed recently.[13,14]

The aim of this paper is to use the asymptotic model derived in Ref. 1 to assess the effects of a variety of stator designs. The model will not only be used as a noise-prediction scheme but also to determine underlying physical mechanisms and identify methods for determining the generic effects of sweep and lean efficiently. The asymptotic model combines the wake evolution scheme with a cascade model,[15] in which the stator is unwrapped at each radius to form a local cascade of blades. This is not strictly two-dimensional strip theory, but a quasi-three-dimensional approach, which accounts for the radial variation of the phase of the incident gust and reconstructs the resulting sound field in the three-dimensional annular duct. The transformation of a swept and leaned stator in the duct geometry to a local cascade is achieved via the transformations described in Ref. 16. Note that, just as in Ref. 16, we do not include the effects of the presence of the outer casing wall when calculating the cascade response, but we will return to this point later.

The upstream-radiated tone noise for an analytical wake profile and a computational-fluid-dynamics (CFD)-generated wake representative of a realistic fan are investigated for a range of stator configurations. It will be shown that an estimate of the generic effects of sweep and lean can be obtained from a simple criterion based solely on the form of the wake at the stator leading edge.

Wake Evolution in Swirling Flow

The wake evolution in the swirling flow region downstream of the rotor is determined using an asymptotic analysis based on large fan-blade number.[1] The region downstream of the rotor is taken to be a uniform axisymmetric annulus. Lengths are nondimensionalized by the tip radius, so that the duct is defined in the region $r_h \le r \le r_t = 1$. The velocity reference scale is the stagnation speed of sound a^*_∞, and subsequently all quantities used are nondimensional unless indicated by superscript $*$.

The total velocity field downstream of the rotor is expressed in terms of a steady, axisymmetric mean flow and a small-amplitude unsteady perturbation of the form

$$\boldsymbol{V}(x, r, \theta, t) = \boldsymbol{U}(r) + \boldsymbol{u}'(x, r, \theta, t) \tag{1}$$

The unsteady velocity perturbation is decomposed into vortical and potential parts[17] so that the unsteady velocity and pressure fields are

written in the form

$$\boldsymbol{u}' = \boldsymbol{u} + \nabla\Phi, \qquad p = -\rho_0 \frac{\mathrm{D}\Phi}{\mathrm{D}t} \tag{2}$$

where $\mathrm{D}/\mathrm{D}t = \partial/\partial t + \boldsymbol{U}\cdot\nabla$ is the convective derivative.

The evolution of the unsteady disturbance is governed by the coupled equations

$$\frac{\mathrm{D}\boldsymbol{u}}{\mathrm{D}t} + (\boldsymbol{u}\cdot\nabla)\boldsymbol{U} = -\boldsymbol{\xi}\times\nabla\Phi \tag{3}$$

$$\frac{\mathrm{D}}{\mathrm{D}t}\frac{1}{a_0^2}\frac{\mathrm{D}}{\mathrm{D}t}\Phi - \frac{1}{\rho_0}\nabla\cdot(\rho_0\nabla)\Phi = \frac{1}{\rho_0}\nabla\cdot(\rho_0\boldsymbol{u}) \tag{4}$$

The wakes shed from the rotor blades give rise to a vortical disturbance, and in mean swirling flow it is appropriate to determine the evolution of this disturbance using an initial-value analysis,[1,18] where the wake distribution at the rotor blade trailing edges provides the initial condition for integration downstream. If the rotor has B blades, then the wake can be decomposed into harmonics, which are integer multiples of the number of fan blades. Typically a fan will have a large number of blades so that the azimuthal mode number $m = NB$ (N an integer) can be treated as a large parameter. If the fan rotates with a nondimensional angular velocity Ω, then the disturbance in the stationary frame is time dependent and of the form

$$[\boldsymbol{u}, \Phi] = [\boldsymbol{A}(x,r), \varphi(x,r)]\exp[imk(r)x + im\theta - i\omega t] \tag{5}$$

where $\omega = m\Omega$ and $mk(r)$ is the axial wave number. The amplitudes depend on both radial and axial locations because in mean swirling flow the disturbance is not purely convected downstream.

In the asymptotic model only dominant (leading order in m) terms are retained in the governing equations. Given that $\omega = \mathcal{O}(m)$ and $\boldsymbol{U} = U_x\boldsymbol{e}_x + U_\theta\boldsymbol{e}_\theta$, the analysis described in Ref. 1 shows that this leads to the definition of the axial wave number as

$$mk(r) = (\omega - mU_\theta/r)/U_x + \mathcal{O}(1) \tag{6}$$

and the governing equations are reduced to three coupled first-order differential equations of the form

$$\frac{\partial\boldsymbol{A}}{\partial x} = \boldsymbol{M}(x,r)\boldsymbol{A} + \mathcal{O}(1/m) \tag{7}$$

where the radius r acts only as a parameter. The matrix $\boldsymbol{M}$ can be read straight off Eqs. (16–19) in Ref. 1. The potential φ is given directly in terms of the vortical velocity $\boldsymbol{A}$ by

$$\varphi = i\frac{x(\mathrm{d}k/\mathrm{d}r)A_r + A_\theta/r + kA_x}{x^2(\mathrm{d}k/\mathrm{d}r)^2 + 1/r^2 + k^2} \tag{8}$$

This is a considerable simplification, and the governing equations can be solved numerically using a simple integration technique. The solution to Eq. (7) is valid in the interior of the flow, but a small boundary-layer correction is required to satisfy the impermeability conditions at the duct walls. This correction is superposed onto the solution of Eq. (7) and decays exponentially away from the duct walls, giving rise to an effective boundary layer of width $\mathcal{O}(1/m)$. The equations satisfied by the boundary-layer correction are given as Eqs. (26–29) in Ref. 1, whereas the condition satisfied by the boundary-layer correction on the duct walls is given by Eq. (25) in Ref. 1. Calculating the correction adds little to the computational complexity of the problem and is described in detail in Ref. 1. Note that it is assumed here that the blade hub-tip ratio is $\mathcal{O}(1)$, so that these $\mathcal{O}(1/m)$-width boundary layers on the inner and outer walls occupy an asymptotically small portion of the span.

The effects of stator design are investigated for two very different wake distributions, both with $B = 26$ rotor blades. One is an analytical profile that expresses the wake as a series of Gaussian curves

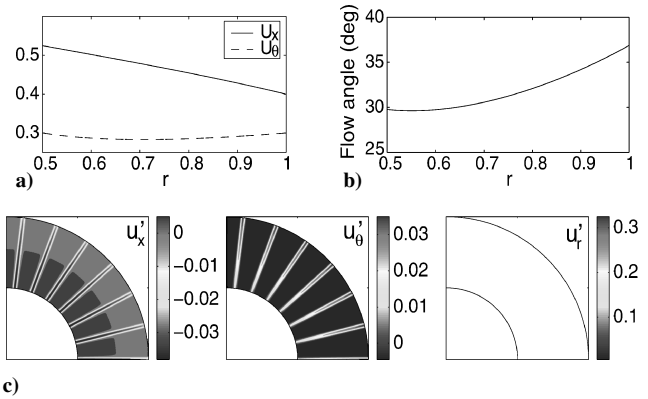

Fig. 2 Initial flow conditions for the Gaussian model fan wake: a) axial U_x and azimuthal U_θ mean flow components; b) mean flow angle; and c) axial, azimuthal, and radial components of fan wake.

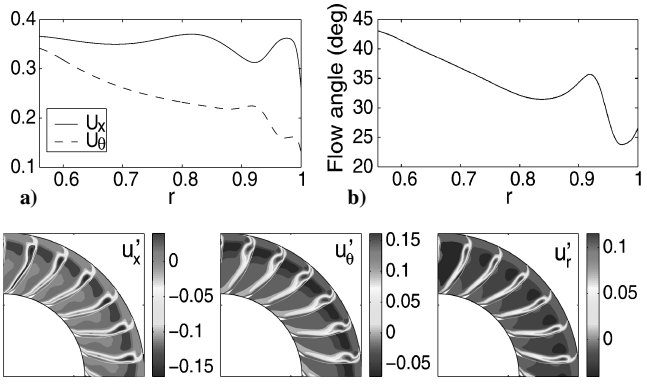

Fig. 3 Initial flow conditions for the CFD fan wake: a) axial U_x and azimuthal U_θ mean flow components; b) mean flow angle; and c) axial, azimuthal, and radial components of fan wake.

centered on each blade trailing edge. The corresponding steady flow is taken to be of the form

$$U_x^2(r) = U_0^2 - 2\left[W_1^2(r^2-1) + 2W_1W_2\,\ell_n(r)\right] \tag{9}$$

$$U_\theta(r) = W_1 r + W_2/r \tag{10}$$

with values $U_0 = 0.4$, $W_1 = 0.2$, $W_2 = 0.1$, and $r_h = 0.5$. The steady and unsteady velocity components are shown in Fig. 2. The second distribution, shown in Fig. 3, is determined from a CFD computation of flow through a genuine rotor configuration.[19]

Wake Interaction with Stator

In this section we will describe how the evolved wake harmonics are matched asymptotically to a local cascade response scheme based on the models in Refs. 15 and 20. Although moving from a three-dimensional geometry to a local two-dimensional system, the approach accounts for any radial dependence in a systematic manner. The local cascade response scheme is an asymptotic calculation based on the assumption of large stator-blade number V. (Because B and V are of the same order, the limits $V \gg 1$ and $B \gg 1$ are equivalent.) This will account for the fast variation along the blade radius of the phase of the incident gusts and for the local variation through the dependence of the mean flow and gust amplitudes on the radius. This will result in the scattered acoustic field having a radial variation that is quite different to the incident gust.

The interaction between the rotor wakes and the stator row is handled by the method of matched asymptotic expansions, as set out in Ref. 1. The unsteady flow generated upstream of the stator can then be expanded as an asymptotic series in powers of $1/V$,

with, for instance, the unsteady pressure being written in the form

$$p^*(r,\theta,x) = p^{(0)^*}(r,\theta,x) + (1/V)p^{(1)^*}(r,\theta,x) + \mathcal{O}(1/V^2) \quad (11)$$

In what follows we only calculate the leading term $p^{(0)^*}$. The duct polar coordinates (r,θ,x) are the so-called outer coordinates, and we take as inner coordinates a local cascade Cartesian system (X^*, Y^*, Z^*), which are related to (x^*, r^*, θ) via a series of transformations,[16] with the resulting X^* axis aligned with the total upstream steady flow. At each representative radius r_0^*, transformations to account for stagger, lean, and sweep are applied to give

$$(X^*, Y^*, Z^*)^T = \boldsymbol{S}\left[V\left(x^* - x_S^*\right), Vr_0^*\theta, V\left(r^* - r_0^*\right)\right]^T \quad (12)$$

where T denotes the vector transpose, x_S^* is the physical location of the stator leading edges, and the transformation matrix $\boldsymbol{S}$ is defined in Appendix A. The factor V on the right-hand side of Eq. (12) has been included to ensure that the cascade leading-edge separation is $\mathcal{O}(1)$ on the scale of the inner coordinate system. Note that these inner coordinates correspond, in the zero sweep and lean case, to the inner coordinates given in Eqs. (39–41) of Ref. 1. The transformations in Eq. (12) do not account for the change in radius between the leading edge and the trailing edge in the transformed system, which leads to a difference in pitch between the leading edge and the trailing edge. This would be significant if determining the noise radiation downstream, but in the case of forward-radiated noise, which is dominated by radiation from the leading edge, this effect can be neglected.

In the duct geometry the stator has semichord length b_d^*, leading-edge separation $\Delta_d^* = 2\pi r^*/V$, stagger angle χ_d, and flow angle $\gamma = \tan^{-1}\{U_\theta(r)/U_x(r)\}$. In the transformed inner cascade system, shown in Fig. 4, the blades have semichord length $b_c^* = Vb_d^*\cos\kappa_s$ (where κ_s is an effective cascade sweep angle defined in Appendix A), leading-edge separation $\Delta_c^* = V\Delta_d^*\sqrt{(S_{12}^2 + S_{22}^2)}$, and cascade stagger angle $\chi_c = \tan^{-1}(S_{12}/S_{22})$. Note that the factor of V in the expressions for b_c^* and Δ_c^* arises from the transformation (12) to the inner coordinates. The transformations for sweep and lean also change the component of the mean velocity normal to the leading edges and introduce a spanwise mean velocity component, which are given, respectively, by

$$U_X^* = U_\infty^*\cos\kappa_s, \qquad U_Z^* = U_\infty^*\sin\kappa_s \quad (13)$$

where $U_\infty^* = [U_x^*(r)^2 + U_\theta^*(r)^2]^{1/2}$. For the cascade model the reference length scale is the blade semichord b_c^*, and the velocity reference scale is the effective upstream steady flow U_X^*. This defines

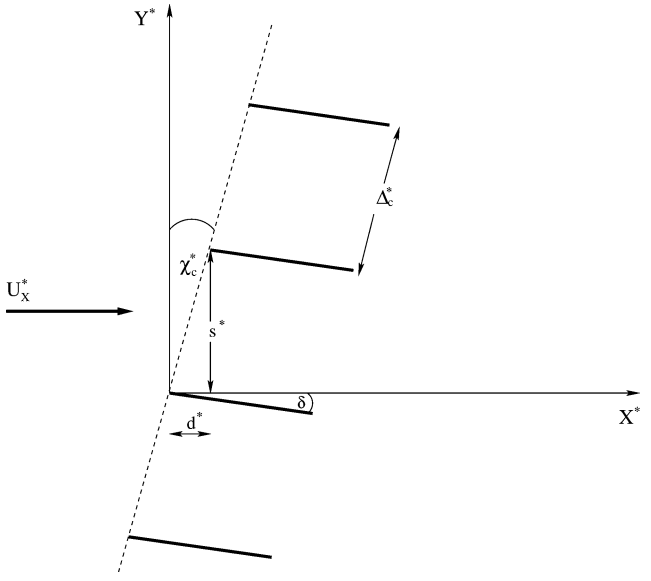

Fig. 4 Local cascade geometry. Z^* axis is out of the page, with mean flow component in this direction U_Z^*.

the relevant Mach number $M = U_X^*/a_0^*$, where a_0^* is the local sound speed.

The unsteady velocity field determined from the wake evolution, which impinges on the stator in the duct, is of the form

$$(\mathcal{A}_x, \mathcal{A}_\theta, \mathcal{A}_r)a_0^* \exp\{i[mk(r)x + m\theta - \omega t]\} \quad (14)$$

with, to leading order in m, $(\mathcal{A}_x, \mathcal{A}_\theta, \mathcal{A}_r)$ given as a sum of contributions from $\boldsymbol{u}$ and $\nabla\Phi$, plus the boundary-layer correction.

In the cascade formulation the unsteady velocity field impinging on the cascade is assumed to have the form

$$(A_X, A_Y, A_Z)U_X^* \exp\{iK[k_X X + k_Y\beta Y + k_Z Z - t]\} \quad (15)$$

where $K = \omega^* b_c^*/U_X^*$ is the aerodynamic reduced frequency (taken to be $\gg 1$) and $\beta^2 = 1 - M^2$. This is a three-dimensional gust, which accounts for the fast radial variation of the gust along the blade radius through the inclusion of the spanwise wave number k_Z in the phase. The gust amplitudes $A_{X,Y,Z}(Z)$ vary slowly in the spanwise direction compared to the phase. Local gradients in gust strength along the blade radius, which must be accounted for at high frequencies,[21] are then incorporated in a consistent asymptotic manner.

The amplitudes and wave numbers in the cascade unsteady velocity field are determined by matching the expressions in Eqs. (14) and (15) using matched asymptotic expansions. The cascade gust amplitudes are then given by

$$(A_X,\ A_Y,\ A_Z)^T = E(r)\boldsymbol{S}(\mathcal{A}_x, \mathcal{A}_\theta, \mathcal{A}_r)^T \quad (16)$$

where

$$E(r) = (1/a_0 M)\exp(imkx_S - imk'x_S r) \times \exp\left[iKr\left(r_t^*/b_c^*\right)(k_X S_{13} + k_Y\beta S_{23} + k_Z S_{33})\right] \quad (17)$$

$a_0 = a_0^*/a_\infty^*$ and $'$ denotes differentiation with respect to r. The corresponding gust wave numbers are given by

$$(k_X, k_Y\beta_\infty, k_Z)^T = (m/K)\left(b_c^*/r_t^*\right)\boldsymbol{T}(k, 1/r, k'x_S)^T \quad (18)$$

where $\boldsymbol{T} = [\boldsymbol{S}^T]^{-1}$. The aerodynamic reduced frequency is related to the duct frequency by $K = \omega b_c^*/Ma_0 r_t^*$. The cascade asymptotic analysis is completed in the limit of high frequency $K \gg 1$.

The cascade model includes the effects of mean loading by defining the blade surface as $Y^* = \delta b_c^* I(X^*)$ for $0 \le X^* \le 2b_c^*$, where the function $I(X^*)$ describes the angle of inclination. It is assumed that $\delta \ll 1$ as in thin airfoil theory so that the steady flow is described as uniform flow with a small nonuniform perturbation. To analyze the distortion of the gust and its subsequent interaction with the cascade, the compressible flow through the cascade in physical space (X^*, Y^*) is transformed into an equivalent incompressible flow through a modified cascade in Prandtl–Glauert space (ϕ, ψ) (Ref. 15). The transformed coordinates ϕ and ψ are nondimensional steady-flow potential and stream-function coordinates, respectively, and are given by

$$\phi = X^*/b_c^* + \delta Re[F] + \mathcal{O}(\delta^2)$$
$$\psi = \beta Y^*/b_c^* + \delta Im[F] + \mathcal{O}(\delta^2) \quad (19)$$

where $\delta b_c^* U_X^* F(X, Y)$ is the complex disturbance potential for the steady flow. The steady disturbance flow is given by $F = F_i/\beta$, where F_i is the equivalent incompressible complex potential. To account for the presence of the spanwise mean flow component U_Z^*, the frame of reference is changed to one moving with this velocity. The unsteady velocity field that interacts with the cascade in (ϕ, ψ) space is then of the form

$$U_X^*(A_X, A_Y, A_Z)\exp(-iK\delta\nu)\exp\{iK[k_X\phi + k_Y\psi + k_Z Z] - i\tilde{K}t\} \quad (20)$$

where $\nu = k_X Re[F] + k_Y Im[F]$, and $\tilde{K} = (1 - k_Z\tan\kappa_s)$.

The upstream acoustic response of the cascade to a single incident gust can be expressed in terms of a modified unsteady velocity potential h, ahead of the cascade, which is composed of a superposition of radiating plane-wave modes in the form[22]

$$h(\phi, \psi) \sim E(r)\exp[-i\delta K(r)\nu(r)] \times \sum_{n=n_1}^{n_2} R_n(r)\exp[-i\sigma_n(r)\phi - i\eta_n(r)\psi] \tag{21}$$

where

$$\sigma_n = \left\{(2n\pi - \sigma')\sin\alpha + \cos\alpha\sqrt{\xi_n}\right\}\Big/\Delta \tag{22}$$

$$\eta_n = \left\{(2n\pi - \sigma')\cos\alpha - \sin\alpha\sqrt{\xi_n}\right\}\Big/\Delta \tag{23}$$

with

$$\xi_n = (\Delta\tilde{K}w)^2 - (2n\pi - \sigma')^2 \tag{24}$$

$$\tan\alpha = \beta\tan(\pi/2 - \chi_c), \qquad \Delta = \sqrt{d^{*2} + \beta^2 s^{*2}}\Big/b_c^* \tag{25}$$

The interblade phase angle σ (determined by periodicity of the incoming gust) and the modified interblade phase angle σ' (determined by periodicity of the dimensional unsteady velocity potential) are given, respectively, by

$$\sigma = \frac{K(k_X d^* + k_Y \beta s^*)}{b_c^*}, \qquad \sigma' = \sigma + \frac{\tilde{K}M^2 d^*}{\left(b_c^*\beta^2\right)} \tag{26}$$

The quantity $\tilde{K}w$ is the acoustic reduced frequency, where

$$w^2 = (M/\beta^2)^2 - (Kk_Z/\tilde{K}\beta)^2 \tag{27}$$

Note that w^2 can be negative if the spanwise wave number Kk_Z is sufficiently large. The values n_1 and n_2 are the lowest and highest values of n such that $\xi_n > 0$, so that each element in the sum in Eq. (21) corresponds to a forward-radiated plane-wave mode propagating in a different direction away from the cascade. The case where the quantity in the square root is zero corresponds precisely to waves propagating along the front face of the cascade.

Some changes to the analysis in Refs. 15 and 20 to determine the radiated sound field in Eq. (21) have been made to account for the inclusion of the wave number k_X (which is unity in the absence of sweep and lean) and for the fact that $\tilde{K} \neq K$ in the incident gust. The effect of these changes on the solution and the exact expression for the modal coefficients R_n are described in Appendix B.

We point out here that we have made the same approximation as Ref. 16, in that the presence of the outer and inner duct walls has been neglected when calculating the cascade response (21). In contrast, the presence of the walls has been included in calculating the incident wake (and will be included when matching the cascade output onto the upstream-going outer pressure field). The effect of the walls on the cascade response (21) will be confined to layers of width $\mathcal{O}(1/m)$ on each wall, and as already noted we are assuming that such layers form only an asymptotically small portion of the vane span. The contribution of this tip (and hub) effect to the total upstream noise will in this case therefore be small but can be expected to become significant either when the leading-order upstream pressure vanishes or when the $\mathcal{O}(1/m)$ layers fill a significant part of the span. In this latter case a different asymptotic approach would be required for both the wake evolution [with the boundary-layer equations (26–29) of Ref. 1 being solved across the full duct span] and the stator response, but this will not be considered in the present paper.

The dimensional acoustic pressure field p_c^* in the stationary frame associated with the sound radiation upstream of the cascade is

$$p_c^*(\phi, \psi, Z) = -\rho_0^* U_X^{*2}\left\{\left[\frac{\partial h}{\partial\phi} - \frac{i\tilde{K}h}{\beta^2}\right] \times \exp\left[iKk_Z Z - i\left(Kt + \tilde{K}\frac{M^2\phi}{\beta^2}\right)\right]\right\} \tag{28}$$

which when transformed back to physical space becomes

$$p_c^*(x, r, \theta) = i\rho_0^* U_X^{*2} E(r)\exp(-iK\delta\nu - iKt)\sum_{n=n_1}^{n_2} R_n(r)\left[\frac{\tilde{K}}{\beta^2} + \sigma_n\right] \times \exp(-i\vartheta_n)\exp\left[iP_n^{(1)}(x - x_S) + iP_n^{(2)}r\theta\right] \tag{29}$$

where

$$\vartheta_n = \left[\sigma_n + \tilde{K}(M^2/\beta^2)\right]\delta Re[F(-\infty)] + \eta_n\delta Im[F(-\infty)] \tag{30}$$

$$P_n^{(j)} = \left(-\left[\sigma_n + \tilde{K}M^2/\beta^2\right]T_{1j} - \eta_n\beta T_{2j} + Kk_Z T_{3j}\right)\left(r_t^*/b_c^*\right) \qquad j = 1, 2 \tag{31}$$

The inner cascade pressure field is now matched onto the outer pressure field upstream in the three-dimensional duct. When this is done, the inner limit of the first term in the large-V expansion (11), $p^{(0)*}$, matches with the far-upstream limit of the cascade field (29). We write the modal expansion of the outer field as

$$p^{(0)*}(x, r, \theta, t) = \rho_\infty^* a_\infty^{*2}\sum_{\hat{m}=-\infty}^{\infty}\sum_{j=1}^{\infty}\hat{c}_{\hat{m}j}\mathcal{P}_{\hat{m}j}(r) \times \exp[i(k_{\hat{m}j}^- x + \hat{m}\theta - \omega t)] \tag{32}$$

where $k_{\hat{m}j}^-$ are the eigenvalues corresponding to nearly sonic modes propagating upstream in mean swirling flow. To determine these eigenvalues and eigenfunctions, the normal-mode expansion is used in the fully coupled acoustic-vorticity equations (3) and (4) to generate an eigenvalue problem. This must be solved numerically and is carried out using a Chebyshev spectral collocation method.[22] The pressure eigenfunctions $\mathcal{P}_{mj}$ are determined from the velocity potential using the relation in Eq. (2). For a given frequency and azimuthal order there are a finite number of propagating (cuton) modes and an infinite number of evanescent (cutoff) modes.

Our aim is to determine the duct azimuthal orders $\hat{m}$ and the unknown pressure coefficients $\hat{c}_{\hat{m}j}$ and thus calculate the upstream noise in the duct. By comparing coefficients of θ in Eqs. (29) and (32), we find that the azimuthal mode number $\hat{m}$ for the acoustic field is related to the cascade wave index n by the Tyler–Sofrin[23] condition

$$\hat{m} = m - nV \tag{33}$$

so that each plane wave mode produced by the cascade corresponds to an azimuthal order in the duct. The modal amplitudes $\hat{c}_{\hat{m}j}$ are then determined from matching the remaining terms in the pressures fields to give

$$\sum_{j=1}^{\infty}\hat{c}_{\hat{m}j}\mathcal{P}_{\hat{m}j}(r)\exp\{ik_{\hat{m}j}^- x_S\} = i\frac{\rho_0^* U_X^{*2}}{\rho_\infty^* a_\infty^{*2}}E(r)e^{-iK\delta\nu} \times R_n(r)\left[\frac{\tilde{K}}{\beta^2} + \sigma_n\right]e^{-i\vartheta_n} \equiv f_n(r) \tag{34}$$

If Eq. (34) is multiplied by $\mathcal{P}_{\hat{m}j}^\dagger(r)$ and integration across the duct radius carried out (where $\dagger$ denotes the complex conjugate), then a matrix equation of the form $\boldsymbol{HC} = \boldsymbol{Q}$ is generated, where $\boldsymbol{C} = [\hat{c}_{\hat{m}1}, \hat{c}_{\hat{m}2}, \ldots]$ and

$$H_{qj} = \int_{r_h}^{1}\mathcal{P}_{\hat{m}q}^\dagger(r)\mathcal{P}_{\hat{m}j}(r)e^{-ik_{\hat{m}j}^- x_S(r)}r\,\mathrm{d}r \tag{35}$$

$$Q_q = \int_{r_h}^{1}\mathcal{P}_{\hat{m}q}^\dagger(r)f_n(r)r\,\mathrm{d}r \tag{36}$$

The modal amplitudes are extracted numerically by truncating the system of equations, where all cuton modes and a sufficient number of cutoff modes are included to ensure convergence of the results.

We must emphasize that the pressure field in the duct upstream of the stator row is given by the full series (11), and we have simply calculated here the first-term approximation to that full series,

valid in the limit of large V. We also wish to emphasize that a range of three-dimensional effects have been included in our analysis of this first term (including the rapid phase variations of the incident gust along the blade span), whereas other three-dimensional effects appear instead at a higher asymptotic order, in the second or higher terms in Eq. (11), and are therefore not included here. Two such effects will be mentioned in particular. First, as already noted, we have neglected the effect of the hub and tip walls on the cascade response. As already stated, these effects will be restricted to layers of width $\mathcal{O}(1/m)$, and because we are explicitly assuming that the span $1-r_h=\mathcal{O}(1)$ it follows that the corresponding contribution to the coefficients Q_q in Eq. (36) is $\mathcal{O}(1/m)$ smaller than the contribution from the main portion of the span. Second, we note that the cutoff cascade modes do not appear in the first term in Eq. (11), but might well have an effect on the second term in Eq. (11), which is where the departures of the blade row response from the local cascade solution will appear.

Results

Validation

To validate this model, a comparison has been made with numerical results in Ref. 13 for scattering of incident disturbances by an annular cascade in a swirling flow (zero sweep and lean). These test cases highlight three-dimensional features of the system such as the radial variation of the mean flow, the effect of incident disturbance coupling with the duct modes on scattering at the stator, and the effect of gust three dimensionality. For the validation, the form of the gust at the duct inlet is

$$u'_x = -\frac{a^{(u)}mU - i\left(U_x^2/\rho_0\right)(\partial/\partial r)[(r\rho_0/U_x)\hat{u}_r]}{krU_x + mU_\theta} \times \exp[i(kx+m\theta-\omega t)] \tag{37}$$

$$u'_\theta = \frac{a^{(u)}krU + i(U_xU_\theta/\rho_0)(\partial/\partial r)[(r\rho/U_x)\hat{u}_r]}{krU_x + mU_\theta} \times \exp[i(kx+m\theta-\omega t)] \tag{38}$$

$$u'_r = \hat{u}_r \exp[i(kx+m\theta-\omega t)] \tag{39}$$

where $U=\sqrt{(U_x^2+U_\theta^2)}$ and U_x and U_θ take the same form as in Eqs. (9) and (10). (Using the notation in Ref. 13, $M_0=U_0$, $M_\Omega=W_1$, and $M_\Gamma=W_2$. Note also that in Ref. 13 the nondimensionalization is based on the mean duct radius r_a^* and values of sound speed and density at this radius.) The inlet is at $x=0$, and the stator leading edge is located at $x=(2b_d^*/r_a^*)\cos\gamma(r_a)$. Numerical values for the magnitude of the upstream acoustic pressure coefficients $\hat{c}_{\hat{m}j}$ are compared for various cases in Tables 1–3. In general two propagating acoustic modes are generated denoted by the radial orders $j=1,2$. Only the first harmonic frequency is considered. Included in the tables are the values of the aerodynamic reduced frequency K and the acoustic reduced frequency Kw; both of these parameters are required to be large for the present asymptotic model to be strictly applicable, but as can be seen reasonable agreement is obtained even for the $\mathcal{O}(1)$ values of K and Kw found here.

In a strictly two-dimensional linear cascade model the spanwise variation of the incident disturbances is maintained by the acoustic modes [i.e., the only spanwise variation is the phase term $\exp(iKk_ZZ)$, which appears in both the incident gust and the scattered acoustic pressure field]. In the present quasi-three-dimensional approach, however, this is no longer the case. The variation of the mean flow and incident gust parameters along the span introduces additional implicit spanwise dependence in the scattered acoustic field. This can be seen explicitly in Eq. (21), in which the cascade wave numbers σ_n, η_n vary with r, so that the radial phase of the cascade field is not simply provided by the gust radial phasing. This allows the model to capture the dominant three-dimensional characteristics of the interaction with an annular cascade, as demonstrated by the reasonable agreement with the numerical results despite the comparatively low values of the asymptotic parameters k and Kw. Note further that reasonable agreement is obtained even in cases in which the incident gust is hub/tip dominated while the radiation mode is tip/hub dominated.

Sweep and Lean Results

Results are presented first for the Gaussian model wake. In this case the stator leading edge at the hub is taken to be at $x=0.3$, the fan rotation rate is $\Omega=0.9$, and the ratio of blade semichord to span is $b_d^*/r_t^*=0.1$.

Table 1 Effect of hub-dominated incident gust on magnitude of upstream acoustic modes $|\hat{c}_{\hat{m}j}|$[a]

Mean flow	j	Atassi et al.[b]	Present results[b]	K	Kw
$M_0=0.4$, $M_\Omega=0$, $M_\Gamma=0$	1	0.040 (t)	0.037 (t)	2.57	1.22
	2	0.073 (h)	0.061 (h)	——	——
$M_0=0.34$, $M_\Omega=0.2107$, $M_\Gamma=0$	1	0.018 (h)	0.019 (h)	2.39–2.90	0.84–1.28
	2	0.025 (h)	0.015 (h)	——	——

[a]Parameters used are $B=20$, $V=24$, $r_h^*/r_t^*=0.5$, $2b_c^*/r_a^*=0.2618$, $\omega=2.5\pi$, $\hat{u}_r=0$, and $a^{(u)}=\cos[\pi/2(r-r_h)/(r_t-r_h)]$.
[b]The letter in parentheses indicates whether the propagating mode is hub dominated (h) or tip dominated (t).

Table 2 Effect of tip-dominated incident gust on magnitude of upstream acoustic modes $|\hat{c}_{\hat{m}j}|$[a]

Mean flow	j	Atassi et al.[b]	Present results[b]	K	Kw
$M_0=0.4$, $M_\Omega=0$, $M_\Gamma=0$	1	0.053 (t)	0.042 (t)	2.57	1.22
	2	0.008 (h)	0.011 (h)	——	——
$M_0=0.34$, $M_\Omega=0.2107$, $M_\Gamma=0$	1	0.030 (h)	0.036 (h)	2.39–2.90	0.84–1.28
	2	0.049 (h)	0.042 (h)	——	——

[a]Parameters used are $B=20$, $V=24$, $r_h^*/r_t^*=0.5$, $2b_c^*/r_a^*=0.2618$, $\omega=2.5\pi$, $\hat{u}_r=0$, and $a^{(u)}=\cos[\pi/2(r_t-r)/(r_t-r_h)]$.
[b]The letter in brackets indicates whether the propagating mode is hub dominated (h) or tip dominated (t).

Table 3 Effect of gust radial velocity on magnitude of upstream acoustic modes $|\hat{c}_{\hat{m}j}|$[a]

Disturbance	j	Atassi et al.	Present results	K	Kw
Two dimensional[b]	1	0.0047	0.0121	3.84–4.24	1.62–1.78
	2	0.0303	0.0295	——	——
Three dimensional[c]	1	0.0039	0.0105	3.84–4.24	1.62–1.78
	2	0.0273	0.0270	——	——

[a]Parameters used are $B=16$, $V=24$, $r_h^*/r_t^*=0.6667$, $2b_d^*/r_a^*=0.3491$, $\omega=3\pi$, $M_0=0.3536$, $M_\Omega=0.1$, $M_\Gamma=0.1$, and $a^{(u)}=1$. [b]Two-dimensional disturbance: $\hat{u}_r=0$. [c]Three-dimensional disturbance: $\hat{u}_r=\sin[\pi(r-r_h)/(r_t-r_h)]$.

At each frequency the wake-stator interaction produces a reflected sound field composing a number of azimuthal orders $\hat{m}$ and a measure of the radiated sound at each BPF is the total cross-sectionally averaged pressure field given by

$$P_m = \int_0^{2\pi} \int_{r_h}^{1} |p_m(x, r, \theta)|^2 r \, \mathrm{d}r \, \mathrm{d}\theta \tag{40}$$

where p_m is the local pressure at frequency $m\Omega$.

The stator stagger angle is taken to be 30 deg and the effects of sweep and lean considered. The cascade calculation determines, at each radius, whether propagating waves are generated by the interaction of the wake with the cascade. If the cuton condition for the cascade

$$(\Delta \tilde{K} w)^2 - (2n\pi - \sigma')^2 > 0 \tag{41}$$

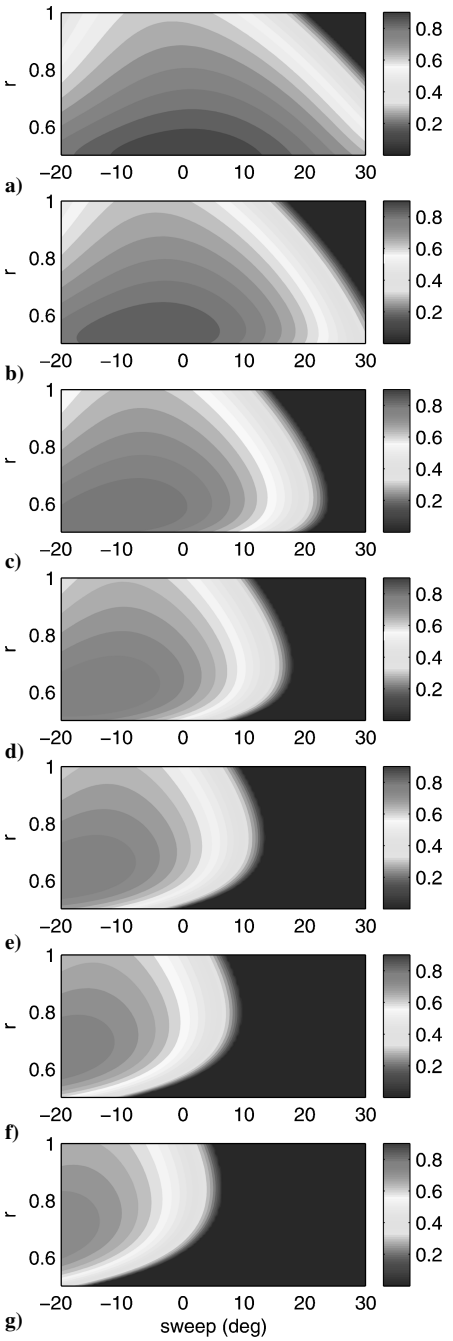

Fig. 5 Contours of w^2 for the Gaussian model wake. For clarity, regions where $w^2 < 0$ have been set to zero: ζ_l = a) −15, b) −10, c) −5, d) 0, e) 5, f) 10, and g) 15 deg.

is examined, then it is clear that this cannot be satisfied if $w^2 < 0$. As noted earlier, the sign of w^2 depends essentially on the magnitude of the spanwise wave number Kk_Z. If $w^2 < 0$ across the whole annulus, then no propagating waves are generated by the cascade interaction, and the leading term $p^{(0)}$ in our expansion (11) of the upstream pressure would vanish. Of course, if $p^{(0)} = 0$ then the upstream pressure is $\mathcal{O}(V)$ smaller than when $p^{(0)} \neq 0$.

The remark at the end of the last paragraph suggests that by examining the behavior of w^2 with sweep and lean angle it is possible to identify optimum conditions for reducing tone noise. This is an extremely simple calculation because it only requires knowledge of the input wave form at the stator leading edges and does not depend on any specific stator characteristics such as the number of vanes, stagger angle, or blade geometry. By examining contours of w^2, it is possible to demonstrate this as shown in Fig. 5. Regions where $w^2 < 0$ are "quieter" regions, in the sense that our leading-order approximation $p^{(0)} = 0$. Figure 5d shows that $p^{(0)} = 0$ for a swept-only stator for sweep angles greater than approximately 18 deg. For positive/negative lean angles this critical sweep angle decreases/increases. This demonstrates that positive lean can enhance the effects of sweep. The sign of w^2 does not provide any information about noise levels, but does provide a clear indication of which sweep and lean combinations will reduce all tones. This criterion, for cutting off all of the local cascade modes, is similar to the criterion given in Ref. 24, which states that no sound is radiated from a rectangular wing encountering an oblique gust when the speed of propagation of the disturbance along the leading edge is subsonic. In the rectilinear case the noise is identically zero when this criterion is satisfied. However, in our problem the noise is nonzero even when $w^2 < 0$ all along the span, but is then given by the second term in Eq. (11) and is smaller by $\mathcal{O}(V)$.

A measure of the stator noise characteristics can be determined by calculations of increasing complexity. Cuton boundaries for specific cascade radiation modes depend on the number of stator blades through the dependence of the cuton condition on Δ and σ'. By definition all of the cascade cuton boundaries must lie within the zone where $w^2 > 0$. As the number of vanes is decreased, the number of cuton modes for each BPF tone increases. This effect is shown in Fig. 6, where twice as many modes are cuton at 1BPF and 2BPF when $V = 30$ compared to a vane count of $V = 50$.

Stator blade geometry, such as angle of attack, blade thickness, and camber, governs the size of the response within the cuton range.

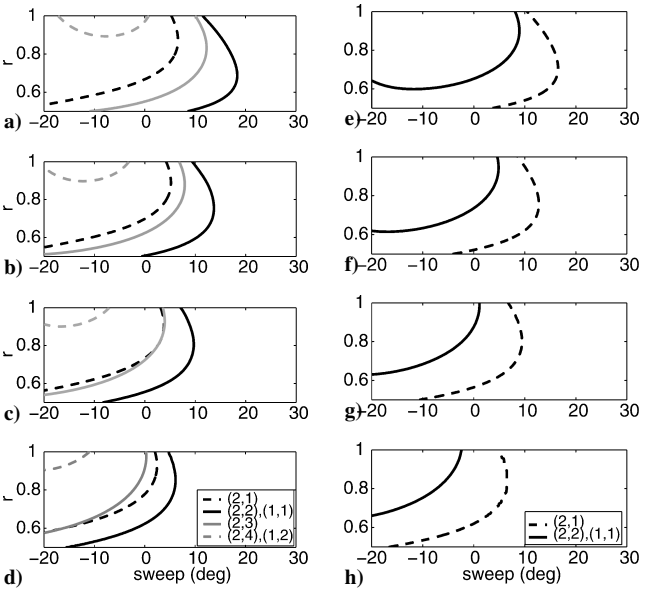

Fig. 6 Cascade cuton boundaries for the Gaussian model wake at 1BPF and 2BPF: a–d) $V = 30$ and e–h) $V = 50$; a) and e) $\zeta_l = 0$ deg; b) and f) $\zeta_l = 5$ deg; c) and g) $\zeta_l = 10$ deg; and d) and h) $\zeta_l = 15$ deg. Labels in the legend boxes denote the modes (BPF, n), where n is the cascade wave index satisfying the cuton condition in Eq. (41). In all cases the cuton region lies to the left of the boundaries.

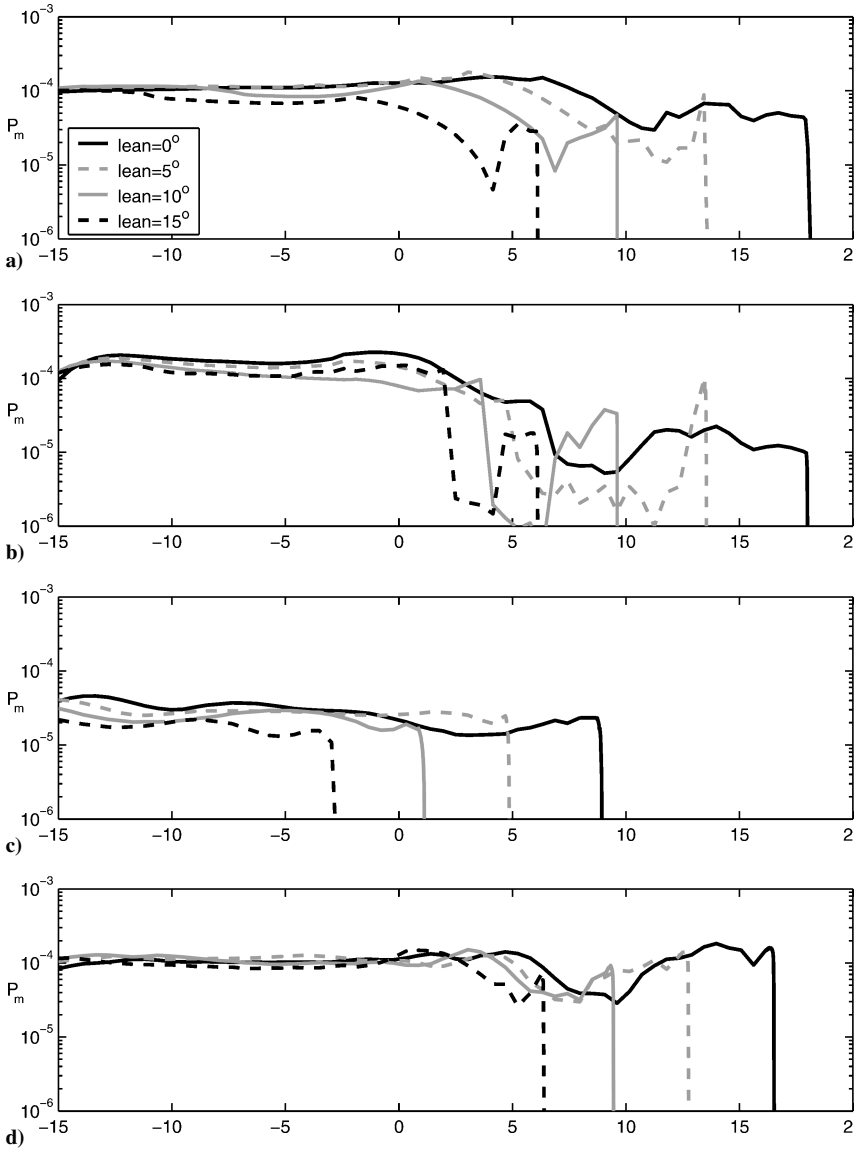

Fig. 7 Large blade number approximation to the noise levels for the Gaussian model wake: a) 1BPF, $V = 30$; b) 2BPF, $V = 30$; c) 1BPF, $V = 50$; and d) 2BPF, $V = 50$.

In Fig. 7 noise levels (with flat-plate representation of the stator blades), which account for the mean loading effects of nonzero angle of attack, are shown. These results confirm that increasing the lean angle brings about earlier cutoff of the cascade modes at the sweep values identified in the Fig. 6. Sharp changes in gradient correspond to an individual cascade mode becoming cut off. Also observe, for positive sweep, a reduction in noise levels as the lean is increased, which results from a reduction in the cascade radiation function R_n. As has already been shown, suitable selection of sweep and lean combinations can reduce the tone noise [by sending $p^{(0)} \to 0$ in Eq. (11)] regardless of the stator blade geometry. The effect of vane count on the noise levels is to change the frequency that generates the largest response. The ability to assess all blade harmonics is important for identifying and targeting the dominant contribution to the total noise field. In Fig. 7 the impulsive reductions to zero amplitude are because we are plotting only the leading term in the upstream pressure. Plots that included the second term in Eq. (11) would not be discontinuous in this way, and cutting off all cascade modes all along the span would definitely not eliminate all tone noise. However, we argue that a relatively steep reduction in the noise level would still be observed around these transition points in the limit of large blade counts.

Our criterion is now applied to the CFD wake[19] (with $\Omega = 0.796$). A more complicated pattern of cascade cuton/cutoff behavior is observed as shown by the contours of w^2 in Fig. 8. This wake has a very strong tip vortex, and consequently larger sweep and lean angles are required to eliminate all of the tones. However, the general trends are the same as for the Gaussian wake with positive lean reinforcing the effects of positive sweep.

Table 4 Values of sweep at which all cascade modes become cut off and the corresponding axial location of the stator tip (x_S^t) for given values of lean[a]

Lean (ζ_l), deg	Critical sweep angle, deg	x_S^t
0	18.0	0.462
5	13.4	0.419
10	9.7	0.385
15	6.5	0.357
——	——	0.71

[a]Last row gives the results for a standard unswept stator.

It is known that the rotor wake becomes increasingly skewed relative to its initial form as it propagates downstream owing to the development of the radial wave number. In the absence of sweep and lean, the local cascade spanwise wave number is related directly to the radial wave number and is responsible for cutting off all cascade modes beyond a critical rotor-stator separation.[1] However, if the critical tip location is determined for a swept and leaned stator then, as shown in Table 4, sweep seems to be much more

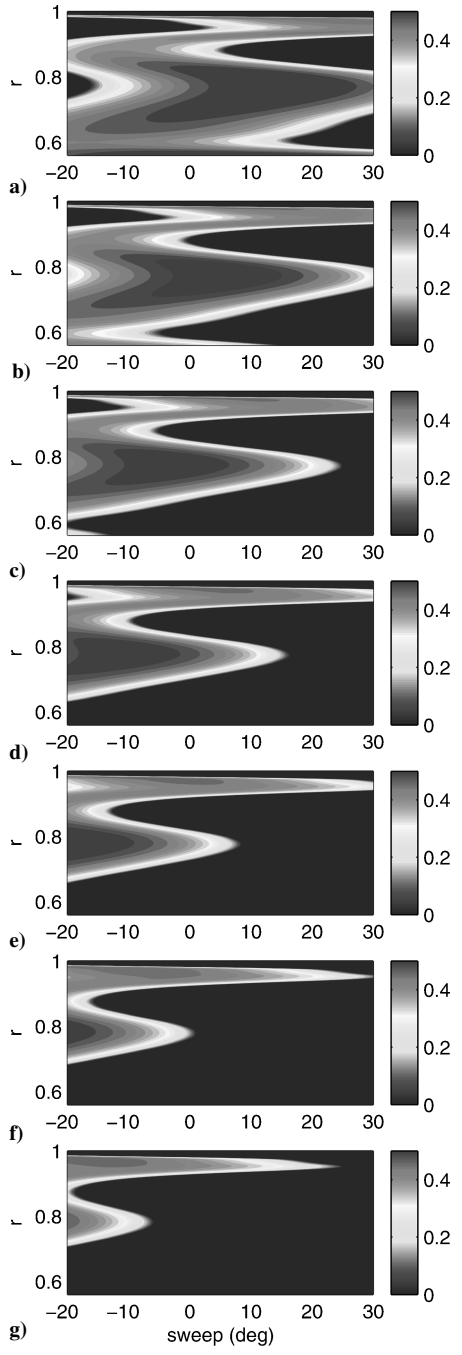

Fig. 8 Contours of w^2 for the CFD wake: ζ_l = a)−30, b) −20, c) −10, d) 0, e) 10, f) 20, and g) 30 deg.

effective than a standard unswept stator (i.e., smaller separations can cutoff modes if the stator is swept). This difference can be attributed to the form of the gust observed by the local cascade. As the duct sweep angle ζ_s is increased, the local cascade sweep and lean angles κ_s and κ_l increase and decrease, respectively. This affects the value of the spanwise wave number Kk_Z as "seen" by the local cascade. Figure 9a shows how the value of k_Z at the stator leading edges increases with both sweep and lean angle. Also shown are the values of k_Z (termed critical values), which render $w^2 = 0$. When these values coincide, all cascade modes become cut off. The critical value of k_Z decreases with both sweep and lean, and it is this feature that makes sweep and lean more effective than simply increasing the rotor-stator separation. These results also indicate how lean enhances the effects of sweep. Similar results for an unswept stator, shown in Fig. 9b, reveal that the critical value of k_Z is constant for all rotor-stator separations, and as a result much larger separations are required before intersection, and cutoff of all cascade modes, occurs.

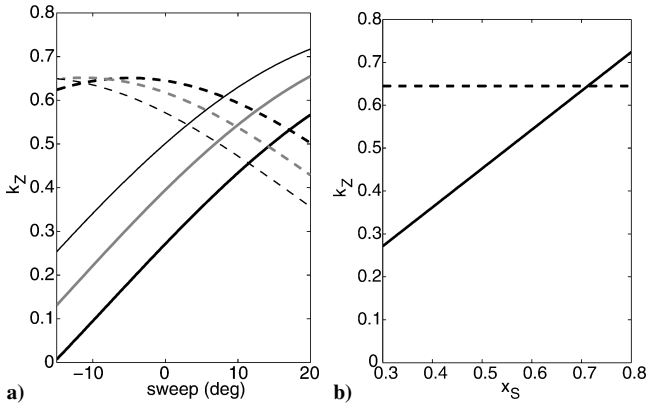

Fig. 9 Variation of spanwise wave number k_Z a) with sweep angle at $r = 0.8$: ——, corresponding to the values of k_Z at the stator leading edges and - - - -, representing the values of k_Z that render $w^2 = 0$. All cascade modes are cut off at the intersection of lines of the same color: thick black line, $\zeta_l = 0$ deg; thick gray line, $\zeta_l = 10$ deg; and thin black line, $\zeta_l = 20$ deg; and b) with rotor-stator separation at $r = 0.8$; —— and - - - -, as for panel a.

Conclusions

An asymptotic method based on large fan-blade number, which accounts for the effects of mean swirling flow, has been applied to the rotor-stator interaction noise problem. This model accounts for aspects of the three-dimensional nature of the flow and geometry and is applied to determine the effects of stator design on upstream-radiated noise. The model couples the three-dimensional wake evolution to a local cascade representation of the stator, which determines the amplitudes of the waves that can propagate away from the cascade at each radius. These cuton cascade waves are then used to reconstruct the acoustic field in the three-dimensional swirling duct flow upstream of the stator. The matching of pressure fields handles the way in which the cascade cuton condition differs from that in an annulus. The cascade cuton condition determines which cascade modes propagate just upstream of the cascade, while the annular cuton condition determines which parts of the radiation escaping the cascade propagate upstream in three dimensions.

A major result of the paper is the identification of a criterion that allows the generic effects of stator sweep and lean to be approximated, based solely on the form of the wake at the stator leading edges. This model predicts the possibility of a significant reduction in rotor-stator interaction tone noise for suitable choice of positive sweep and lean.

The model described in this paper could be used to undertake a comprehensive investigation into rotor-stator interaction noise, which would be of use in the early stages of design. It is possible to determine the noise response at a number of harmonic frequencies across a wide range of fan operating conditions, flow conditions, and stator configurations. The results presented in this paper support the idea of using a low-vane count stator to reduce broadband noise,[16] with sweep and lean applied in optimal combination to maximize the reduction of the tonal component.

Appendix A: Transformation Matrix

The duct flow, lean and sweep angles, γ, ζ_l, and ζ_s, respectively, define effective lean κ_l and sweep κ_s rotation angles in the cascade. The relationship between these angles was derived by Hanson[16] and is given by

$$\tan\kappa_l = \cos\gamma\tan\zeta_l - \sin\gamma\tan\zeta_s \tag{A1}$$

$$\tan\kappa_s = \cos\kappa_l(\sin\gamma\tan\zeta_l + \cos\gamma\tan\zeta_s) \tag{A2}$$

The coordinate transformation matrix relating duct to cascade coordinates is

$$\boldsymbol{S} = \begin{bmatrix} \cos\gamma\cos\kappa_s + \sin\gamma\sin\kappa_l\sin\kappa_s & \sin\gamma\cos\kappa_s - \cos\gamma\sin\kappa_l\sin\kappa_s & -\cos\kappa_l\sin\kappa_s \\ -\sin\gamma\cos\kappa_l & \cos\gamma\cos\kappa_l & -\sin\kappa_l \\ \cos\gamma\sin\kappa_s - \sin\gamma\sin\kappa_l\cos\kappa_s & \sin\gamma\sin\kappa_s + \cos\gamma\sin\kappa_l\cos\kappa_s & \cos\kappa_l\cos\kappa_s \end{bmatrix} \tag{A3}$$

Appendix B: Leading-Edge Source

This Appendix describes the solution for the modified potential $h(\phi, \psi)$, which is given in Eq. (21). Myers and Kerschen[25] showed that the modified potential is governed by a perturbation to the Helmholtz equation. The inclusion of sweep and lean gives rise to changes to the incident gust (i.e., $k_X \neq 1$, $\tilde{K} \neq K$) and subtle changes to the cascade response. In this case the dimensional unsteady velocity potential G' for the problem is assumed to have the form

$$G' = U_X^* b_c^* h(\phi, \psi) \exp\{iKk_Z Z - i\tilde{K}[t + M^2\phi/\beta^2] + \delta M^2 q(\phi, \psi)\} \tag{B1}$$

where $\delta U_X^* q$ is the dimensional perturbation to the flow speed U_X^*. This reduces to the Myers and Kerschen form when $\tilde{K} \to K$ (i.e., zero sweep and lean). The equation governing the modified potential takes the form

$$(\nabla^2 + \tilde{K}^2 w^2 + \delta\mathcal{L}_1)(h) = \delta\tilde{K}\tilde{S}(\phi, \psi) e^{i\tilde{K}\tilde{\Omega}} \tag{B2}$$

The operator $\mathcal{L}_1$ is that given in Eq. (2.4d) of Ref. 25 and the perturbation source term $\tilde{K}\tilde{S}(\phi, \psi) = KS(\phi, \psi)$ with $S(\phi, \psi)$ defined in Eq. (2.5a) of Ref. 25, and with k replaced by $\tilde{K}$ in both cases. The phase in the source term is

$$\tilde{K}\tilde{\Omega} = (Kk_X + M^2/\tilde{K}\beta^2)\phi + Kk_Y\psi + Kg(\phi, \psi) \tag{B3}$$

where $g(\phi, \psi)$ is Lighthill's drift function defined in Eq. (2.5c) of Ref. 25.

The boundary condition describing zero normal velocity on the blade surfaces becomes

$$\frac{\partial h}{\partial \psi} + \delta M^2 \frac{\partial q}{\partial \psi} h = -\left[\frac{A_Y}{\beta^2}(1 - \delta M^2 q) - \delta 2 A_X \mu\right] e^{i\tilde{K}\hat{\Omega}} \tag{B4}$$

It is shown in Ref. 25 that the sound radiated forward from each blade is determined by a series of matched asymptotic expansions with inner regions around each blade leading edge and an outer region elsewhere. A full mathematical derivation of the radiated sound field is given in Ref. 25 for an isolated airfoil and in Refs. 15 and 20 for a cascade. Following this method, the radiation from the leading edge of the zeroth blade in the cascade gives rise to a modified potential of the form

$$h_0(\phi, \psi) = \frac{D(\Theta; A_Y, A_X)}{\tilde{K}^{\frac{3}{2}}\mathcal{R}^{\frac{1}{2}}} \exp\{i\tilde{K}[w\mathcal{R} + \delta P(\mathcal{R}, \Theta) + \delta g]\} \tag{B5}$$

where $\mathcal{R} = (\phi^2 + \psi^2)^{1/2}$ and $\Theta = \tan^{-1}(\psi/\phi)$ are polar coordinates, δg represents the phase distortion, or drift, experienced by the gust in propagating from upstream infinity to the leading edge, and $\delta P(\mathcal{R}, \Theta)$ represents the phase distortion of the ray field as a result of its propagation through the nonuniform outer flow. The directivity function $D(\Theta; A_Y, A_X)$ is composed of the directivity for the radiation from the leading edge of a flat plate (D_0) plus an $\mathcal{O}(\delta\tilde{K}^{1/2})$ contribution, which represents the effects of the symmetric and antisymmetric components of the nonuniform mean flow, so that

$$D(\Theta) = D_0(\Theta) + \delta\tilde{K}^{\frac{1}{2}}[D_1(\Theta) + D_2(\Theta) + D_3(\Theta)] \tag{B6}$$

The change in the incident gust brought about by sweep and lean manifests itself in the acoustic response through the directivity functions $D_{0,\ldots,3}$ as follows:

$$D_0(\Theta) = \frac{A_Y e^{-i\pi/4}\cos(\Theta/2)}{\beta\pi^{\frac{1}{2}}(w\cos\Theta - \xi)(\xi + w)^{\frac{1}{2}}} \tag{B7}$$

with $\xi = (Kk_X/\tilde{K} + M^2/\beta^2)$,

$$D_1(\Theta) = \frac{i2A_Y}{\beta^2 w^{\frac{1}{2}}(\xi - w\cos\Theta)^{\frac{1}{2}}} \tag{B8}$$

$$D_2(\Theta) = D_{2p}(\Theta) + D_{2c}(\Theta) \tag{B9}$$

where

$$D_{2p}(\Theta) = \frac{-i(\xi - w\cos\Theta) f_1(-w\cos\Theta) + \tilde{k}_Y f_2(-w\cos\Theta)}{4\left(\xi^2 + \tilde{k}_Y^2\right)[2w(\xi - w\cos\Theta)]^{\frac{1}{2}}(\lambda_1 + w\cos\Theta)(\lambda_2 + w\cos\Theta)} \tag{B10}$$

$$D_{2c}(\Theta) = -\left[4(\lambda_1 - \lambda_2)(i\tilde{k}_Y C_4 + i\xi C_3) + \frac{(\lambda_1 + w)^{\frac{1}{2}} f_2(\lambda_1)}{(\lambda_1 + \xi)^{\frac{1}{2}}(\lambda_1 + w\cos\Theta)} - \frac{(\lambda_2 + \xi) f_2(\lambda_2) + i\tilde{k}_Y f_1(\lambda_2)}{[(\lambda_2 - w)(\lambda_2 + \xi')]^{\frac{1}{2}}(\lambda_2 + w\cos\Theta)}\right] \frac{\cos(\Theta/2)}{4(\lambda_1 - \lambda_2)\left(\xi^2 + \tilde{k}_Y^2\right)} \tag{B11}$$

with $\tilde{k}_Y = Kk_Y/\tilde{K}$ and

$$C_1 = i2^{\frac{3}{2}}(K/\tilde{K})\left(A_X/\beta^3 - k_Y A_Y\right)$$

$$C_2 = i2^{\frac{3}{2}}(K/\tilde{K})\left(k_Y A_X/\beta + A_Y/\beta^2\right) \tag{B12}$$

$$C_3 = -\sqrt{2}(K/\tilde{K})^2\left(A_X M^2/\beta^3\right)$$

$$C_4 = -\sqrt{2}(K/\tilde{K})^2\left(A_Y M^2/\beta^2\right) \tag{B13}$$

The functions $f_{1,2}$ are given by

$$f_1(\lambda) = [iC_2 - 2C_4(\lambda + \xi)]\left(-\xi^2 + \tilde{k}_Y^2 - w^2 - 2\xi\lambda\right) + [C_1 + 2iC_3(\lambda + \xi)]2i\tilde{k}_Y(\lambda + \xi) \tag{B14}$$

$$f_2(\lambda) = [iC_2 - 2C_4(\lambda + \xi)]2i\tilde{k}_Y(\lambda + \xi) + [C_1 + 2iC_3(\lambda + \xi)]\left(-\xi^2 + \tilde{k}_Y^2 - w^2 - 2\xi\lambda\right) \tag{B15}$$

where

$$\lambda_{1,2} = \frac{\xi}{2}\left[\frac{\xi^2 + \tilde{k}_Y^2 + w^2}{\xi^2 + \tilde{k}_Y^2}\right] \pm \frac{i\tilde{k}_Y}{2}\left[\frac{\xi^2 + \tilde{k}_Y^2 - w^2}{\xi^2 + \tilde{k}_Y^2}\right] \tag{B16}$$

$$D_3(\Theta) = \frac{iA_Y}{[w(\xi - w\cos\Theta)]^{\frac{1}{2}}}\left[1 - \frac{M^2}{\beta^2} - \frac{\xi}{\xi - w\cos\Theta}\right] + \frac{iA_Y(\gamma + 1)M^4}{w^{\frac{3}{2}}(\xi + w)^{\frac{1}{2}}\beta^4}\left[\frac{\beta^{-2}}{2}\cos\Theta - \frac{w}{4}\cos 2\Theta\right] \tag{B17}$$

In the final form of the modified potential , the modal amplitudes in Eq. (21) are uniformly valid[20] with the new directivity functions (just defined) incorporated and are given explicitly by

$$R_n(\Theta_n) = \frac{e^{i\pi/4}(2\pi)^{\frac{1}{2}}\exp[i\tilde{K}\delta p_1(\Theta_n) + i\tilde{K}\delta g]}{\Delta\tilde{K}^2 w^{\frac{1}{2}}\sin(\Theta_n - \alpha)} D(\Theta_n)\mathcal{F}(\Theta_n) \tag{B18}$$

where

$$\Theta_n = \alpha + \cos^{-1}\left\{\frac{\sigma' - 2n\pi}{\Delta \tilde{K} w}\right\} \tag{B19}$$

$\delta \tilde{K}\, p_1(\Theta_n)$ and $\mathcal{F}(\Theta_n)$ are given, respectively, by Eqs. (3.13) and (3.21) in Ref. 20.

Acknowledgments

A. J. Cooper acknowledges the financial support provided by The Royal Society. The authors are also very grateful to A. Ferrecchia for providing the numerical wake data.

References

[1]Cooper, A. J., and Peake, N., "Upstream-Radiated Rotor-Stator Interaction Noise in Mean Swirling Flow," *Journal of Fluid Mechanics*, Vol. 523, 2005, pp. 219–250.

[2]Envia, E., and Nallasamy, M., "Design Selection and Analysis of a Swept and Leaned Stator Concept," *Journal of Sound and Vibration*, Vol. 228, No. 4, 1999, pp. 793–836.

[3]Adamczyk, J. J., "Passage of a Swept Air Foil Through an Oblique Gust," *Journal of Aircraft*, Vol. 11, No. 5, 1974, pp. 281–287.

[4]Envia, E., and Kerschen, E. J., "Noise Produced by the Interaction of a Rotor Wake with a Swept Stator Blade," AIAA Paper 84-2326, Oct. 1984.

[5]Envia, E., and Kerschen, E. J., "Noise Generated by Convected Gusts Interacting with Swept Airfoil Cascades," AIAA Paper 86-1872, July 1986.

[6]Envia, E., and Kerschen, E. J., "Influence of Vane Sweep on Rotor-Stator Interaction Noise," NASA CR-187052, Dec. 1990.

[7]Glegg, S. A. L., "The Response of a Swept Blade Row to a Three-Dimensional Gust," *Journal of Sound and Vibration*, Vol. 227, No. 1, 1999, pp. 29–64.

[8]Schulten, J. B. H. M., "Vane Sweep Effects on Rotor/Stator Interaction Noise," *AIAA Journal*, Vol. 35, No. 6, 1997, pp. 945–951.

[9]Rao, G. V. R., "Use of Leaning Vanes for Fan Noise Reduction," AIAA Paper 72-126, Jan. 1972.

[10]Kazin, S. B., "Radially Leaned Outlet Guide Vanes for Fan Source Noise Reduction," NASA CR-134486, Nov. 1973.

[11]Schulten, J. B. H. M., "Sound Generated by Rotor Wakes Interacting with a Leaned Stator Vane," *AIAA Journal*, Vol. 20, No. 10, 1982, pp. 1352–1358.

[12]Woodward, R. P., Elliot, D. M., Hughes, C. E., and Berton, J. J., "Benefits of Swept-and-Leaned Stators for Fan Noise Reduction," *Journal of Aircraft*, Vol. 38, No. 6, 2001, pp. 1130–1138.

[13]Atassi, H. M., Ali, A. A., Atassi, O. V., and Vinogradov, I. V., "Scattering of Incident Disturbances by an Annular Cascade in a Swirling Flow," *Journal of Fluid Mechanics*, Vol. 499, 2004, pp. 111–138.

[14]Elhadidi, B., and Atassi, H. M., "High Frequency Sound Radiation from an Annular Cascade in Swirling Flows," AIAA Paper 2002-2559, June 2002.

[15]Peake, N., and Kerschen, E. J., "Influence of Mean Loading on Noise Generated by the Interaction of Gusts with a Flat-Plate Cascade: Upstream Radiation," *Journal of Fluid Mechanics*, Vol. 347, 1997, pp. 315–346.

[16]Hanson, D. B., "Theory for Broadband Noise of Rotor and Stator Cascades with Inhomogeneous Inflow Turbulence Including Effects of Lean and Sweep," NASA CR-2001-210762, May 2001.

[17]Goldstein, M. E., "Unsteady Vortical and Entropic Distortions of Potential Flows Around Arbitrary Obstacles," *Journal of Fluid Mechanics*, Vol. 89, 1978, pp. 433–468.

[18]Golubev, V. V., and Atassi, H. M., "Unsteady Swirling Flows in Annular Cascade, Part 1: Evolution of Incident Disturbances," *AIAA Journal*, Vol. 38, No. 7, 2000, pp. 1142–1149.

[19]Ferrecchia, A., Dawes, W. N., and Dhanasekaran, P. C., "Compressor Rotor Wakes and Tone Noise Study," AIAA Paper 2003-3328, May 2003.

[20]Evers, I., and Peake, N., "On Sound Generation by the Interaction Between Turbulence and a Cascade of Airfoils with Non-Uniform Mean Flow," *Journal of Fluid Mechanics*, Vol. 463, 2002, pp. 25–52.

[21]Majumdar, S. J., and Peake, N., "Three-Dimensional Effects in Cascade-Gust Interaction," *Wave Motion*, Vol. 23, No. 4, 1996, pp. 321–337.

[22]Cooper, A. J., and Peake, N., "Propagation of Unsteady Disturbances in a Slowly-Varying Duct with Mean Swirling Flow," *Journal of Fluid Mechanics*, Vol. 445, 2001, pp. 207–234.

[23]Tyler, J. M., and Sofrin, T. G., "Axial Flow Compressor Noise Studies," *SAE Transactions*, Vol. 70, 1962, pp. 309–332.

[24]Martinez, R., and Widnal, S. E., "Unified Aerodynamic–Acoustic Theory for a Thin Rectangular Wing Encountering a Gust," *AIAA Journal*, Vol. 18, No. 6, 1980, pp. 636–645.

[25]Myers, M. R., and Kerschen, E. J., "Influence of Incidence Angle on Sound Generation by Airfoils Interacting with High-Frequency Gusts," *Journal of Fluid Mechanics*, Vol. 292, 1995, pp. 271–304.

H. Atassi
Associate Editor